CrossMark

A Better Reconciliation of Hubble Tension in the Dark Energy Scalar Field

Le Fu[1], Li Chen[2], Maoyou Yang[2], Junmei Wang[2], and Ming-Jian Zhang[2]

[1] School of Information and Automation Engineering, Qilu University of Technology (Shandong Academy of Sciences), Jinan 250353, China
[2] International School for Optoelectronic Engineering, Qilu University of Technology (Shandong Academy of Sciences), Jinan 250353, China
zhangmj@mail.bnu.edu.cn

Abstract

Hubble tension between the local measurement and global observation has been a key problem in cosmology. In this paper, we consider the quintessence scalar field, phantom field and quintom field as the dark energy to reconcile this problem. Different from most previous work, we start from the dimensionless equation of state (w) of dark energy, not a parameterization of potential. The combined analysis shows that observational data sets favor Hubble constant $H_0 = 71.3^{+0.854}_{-0.917}$ km s^{-1} Mpc^{-1}, which can reconcile Hubble tension within 1.20σ. We also perform a Bayes factor analysis using the `MCEvidence` code, and confirm that the phantom scalar field is still the most effective. To investigate the reason of Hubble tension, we analyze the density parameter. The comparison shows that the scalar fields provide a slightly larger $\Omega_b h^2$ and smaller $\Omega_c h^2$ than the standard ΛCDM model. We finally analyze a possible reason of Hubble tension from the kinematic acceleration $\ddot{a}$. We find an interesting physical phenomenon. The acceleration $\ddot{a}$ in these scalar fields are similar as the ΛCDM model at about redshift $z > 0.5$. However, they increase and deviate from each other at low redshift, especially in the near future. Only the $\ddot{a}$ in phantom scalar field will decrease in the future.

Key words: (cosmology:) dark energy – (cosmology:) cosmological parameters – cosmology: theory

1. Introduction

The secular ΛCDM model in explaining the cosmic acceleration, favors well against the large spans of cosmological data. With the improvement of volume and accuracy of observational data, however, discrepancies of some cosmological parameters in this model become increasingly serious. Especially, tension of Hubble constant H_0 between the global and local measurement presents a statistical significance. In the latest local measurement (Riess et al. 2021), SH0ES Team issued $H_0 = 73.2 \pm 1.3$ km s^{-1} Mpc^{-1} at 68% CL with 1.8% uncertainty (hereafter R20) using the Cepheids observations. However, global temperature spectrum of cosmic microwave background (CMB) for Planck2018 (Aghanim et al. 2020) present $H_0 = 67.27 \pm 0.60$ km s^{-1} Mpc^{-1} at 68% CL in the flat ΛCDM scenario. Their differences have increased to be a 4.2σ. This problem is commonly called "Hubble tension."

Hubble constant is important to our cosmological research. It does not only play a vital influence on determination of cosmic age, but dominate the physical process such as comic nucleosynthesis and growth of cosmic structure. We also have affirmed that Hubble constant inevitably affects dark energy reconstruction (Zhang & Li 2018). Even, Freedman (2017) believed that Hubble tension may indicate a new physics. The Hubble constant, therefore, is an important observational target for a long time.

The observation of Hubble constant is technically difficult. Primarily, it was estimated from the Hubble law $v = H_0 d$, a linear relationship between recession velocity of galaxies and distance. The first Hubble constant H_0 is about 500 km s^{-1} Mpc^{-1} (Hubble & Humason 1931). This large value is due to the confusion of two generations of pulsating stars in calculation of distance standards. Sandage demonstrated this mistake and revised H_0 down to 75 km s^{-1} Mpc^{-1}. Accurate distance measurement has always been a problem in the Hubble constant program. In 1921, Leavitt & Pickering (1912) found that the period of brightness fluctuation of Cepheid variables is highly regular, i.e., period–luminosity relation. Cepheids thereafter is used as the standard candles. Hubble constant from the SH0ES Team is just based on this method. Till now, a number of other tools are available, such as the Tip of Red Giant Branch, Surface Brightness Fluctuation, Maser in galaxy NGC 4258, gravitational lens time delays, and fashionable gravitational wave (GW). However, there are also differences between them. For example, the updated Tip of Red Giant Branch obtains $H_0 = 69.8 \pm 0.6$(stat) ± 1.6(sys) km s^{-1} Mpc^{-1} (Freedman 2021). Meanwhile, the GW observations support a larger value.

The Hubble tension rapidly attracted widespread attention (Wu et al. 2021; Yang et al. 2021b; Ye et al. 2021; Zhao et al. 2021). As Freedman (2017) argued that we are at a crossroad in cosmology. Hubble tension is signaling new physics or unrecognized uncertainties. If not due to the systematic errors, it would indicate a failure of cosmological standard model. Till now, a number of models (see Di Valentino et al. 2021a for a review) were proposed to reconcile the Hubble tension, involving early and late dark energy, modified gravity,

inflationary models and so on. In Niedermann & Sloth (2020), the authors investigated a new early dark energy model using the data sets Planck2018+CMB lensing+BAO+Pantheon, finding that $H_0 = 69.6^{+1.0}_{-1.3}\,\mathrm{km\,s^{-1}\,Mpc^{-1}}$, which can resolve the Hubble tension within 2.3σ. For the famous CPL dark energy, Planck2018 + Pantheon + BAO provided $H_0 = 68.31 \pm 0.82\,\mathrm{km\,s^{-1}\,Mpc^{-1}}$ (Aghanim et al. 2020), a 3.2σ tension with R20. However, we note that a phenomenologically emergent dark energy with $w = -1 - \frac{1}{3\ln 10}[1 + \tanh(\log_{10}(1+z))]$ (Li & Shafieloo 2019; Yang et al. 2021a) can optimistically improve the Hubble tension. Considering the full CMB analysis in this model, Planck2015 alone can give $H_0 = 72.58^{+0.79}_{-0.80}\,\mathrm{km\,s^{-1}\,Mpc^{-1}}$ (Pan et al. 2020), which has improved the tension to 1σ. Similarly, for an exponential form modified gravity $f(\mathcal{T}) = -\mathcal{T}e^{\beta(\mathcal{T}_0/\mathcal{T})}$, Planck2018 + CMB lensing + BAO gives $H_0 = 71.49 \pm 0.47\,\mathrm{km\,s^{-1}\,Mpc^{-1}}$, at 1.2σ tension. Interestingly, vacuum metamorphosis model motivated by the quantum gravitational effects can provide a much large estimation, $H_0 = 81.1 \pm 2.1\,\mathrm{km\,s^{-1}\,Mpc^{-1}}$ by the single Planck2018 fitting (Di Valentino et al. 2020). On the whole, Hubble tension can be resolved ranging from 1σ to 4σ level (Di Valentino et al. 2021a).

In the present paper, we would like to return the Hubble tension in the scalar field dark energy. We consider the quintessence field, phantom field and quintom field. For the scalar field study, an inevitable problem is the modeling of potential $V(\phi)$ over scalar field ϕ. Generally, potential V was understood via parameterization, such as power-law potential $V(\phi) \propto \phi^p$, exponential potential $V(\phi) \propto e^{-\lambda\phi}$. However, we note that parameter H_0 is usually hidden in potential $V(\phi)$, which greatly increases the difficulty of numerical calculations. In this paper, we rebuild the potential V from the equation of state (EoS w) of late dark energy, a dimensionless parameter, which can break above difficulties. For the quintessence field $\phi(t)$ and phantom field $\sigma(t)$, we construct a simplified version basing on the Cai et al. (2007a). Our constraints show that one model can reconcile the Hubble tension at a better level.

This article is organized as follows: In Section 2, we introduce the scalar field. In Section 3 we describe the relevant data we use. We present the reconstruction result, and explore the reason in Section 4. Finally, in Section 5 conclusion and discussion are drawn.

2. Scalar Field Theory

In coming section, we will introduce the construction of scalar field, namely, quintessence field, phantom field and quintom field.

We take into account a spatially flat Friedmann–Robertson–Walker universe with matter and scalar field. The dynamical

Friedmann equation can be expressed as follows

$$H^2 = \frac{8\pi G}{3}(\rho_m + \rho_\phi), \tag{1}$$

where $H = \dot{a}/a$ is the Hubble expansion rate. Considering dark matter energy density $\rho_m = \rho_{m0}(1+z)^3$, we have its density parameter $\Omega_{m0} = \rho_{m0}/\rho_{c0}$, where $\rho_{c0} = 3H_0^2/(8\pi G)$ is the critical density. For the quintessence scalar field ϕ, its energy density and pressure are defined as

$$\rho_\phi = \frac{1}{2}\dot{\phi}^2 + V(\phi),$$
$$p_\phi = \frac{1}{2}\dot{\phi}^2 - V(\phi), \tag{2}$$

where the dot represents derivative with respect to cosmic time t over field ϕ. To solve this dynamical equation, generally, the potential V should be constructed via the parameterization of scalar field, such as power-law potential $V(\phi) \propto \phi^p$, exponential potential $V(\phi) \propto e^{-\lambda\phi}$, inverse power-law potential $V(\phi) \propto \phi^{-p}$, inverse exponential potential $V(\phi) \propto e^{\lambda/\phi}$, double exponential potential $V(\phi) \propto V_1 e^{-\lambda_1\phi} + V_2 e^{-\lambda_2\phi}$, Hilltop potential $V(\phi) \propto \cos(\phi)$. Meanwhile, some other complex models can also be found in Sahni (2004), such as $e^{\lambda\phi^2}/\phi^\alpha$, $(\cosh\lambda\phi - 1)^p$, $\sinh^{-\alpha}(\lambda\phi)$, $[(\phi - B)^\alpha + A]e^{-\lambda\phi}$. However, we note that the parameter H_0 is hidden in potential $V(\phi)$. It greatly increases the difficulty of numerical calculations. To break this dilemma, we rebuild the potential V from the equation of state w of scalar field dark energy, a dimensionless parameter.

The EoS parameter for quintessence scalar field is

$$w = \frac{p_\phi}{\rho_\phi}. \tag{3}$$

Combining with Equation (2), we can obtain the potential

$$V = \frac{1}{2}\frac{1-w}{1+w}\dot{\phi}^2. \tag{4}$$

Finally, we have the Hubble parameter

$$H^2(z) = H_0^2 \Omega_{m0}(1+z)^3 + \frac{8\pi G}{3}\frac{\dot{\phi}^2}{1+w}. \tag{5}$$

As long as the scalar field ϕ and w are available, the Hubble parameter can be logically solved. Moreover, solution of Hubble constant becomes easier. In the present paper, we consider a fractional form $w = w_0 + w_1 z/(1+z)^2$ and logarithmic form $w = w_0 + w_1 \ln(1+z)/(1+z)$. For the quintessence dark energy, $w > -1$ should be satisfied.

For the phantom scalar field σ, its energy density and pressure are

$$\rho_\sigma = -\frac{1}{2}\dot{\sigma}^2 + V(\sigma),$$

$$p_\sigma = -\frac{1}{2}\dot{\sigma}^2 - V(\sigma). \tag{6}$$

Different from the quintessence field, the minus sign—is in derivative $\dot{\sigma}^2$. Following the above operation, we obtain the Hubble parameter

$$H^2(z) = H_0^2 \Omega_{m0}(1+z)^3 + \frac{8\pi G}{3}\frac{-\dot{\sigma}^2}{1+w}. \tag{7}$$

Similarly to quintessence scalar field, the Hubble parameter can be solved logically, as long as the scale fields σ and w are available. However, we should notice that EoS is $w < -1$ in this scalar field.

For the quintom field, it is a combination of quintessence field and phantom field. With the cosmic evolution, the quintessence field can transfer into phantom field, or the phantom field transfers into quintessence field. A number of theoretical works were investigated (Zhao et al. 2005; Cai et al. 2007b, 2010). Similarly, the Hubble parameter can be expressed as

$$H^2(z) = H_0^2 \Omega_{m0}(1+z)^3 + \frac{8\pi G}{3}\frac{\dot{\phi}^2 - \dot{\sigma}^2}{1+w}. \tag{8}$$

With regard to the reconstruction of scalar field $\phi(t)$ and $\sigma(t)$, Cai et al. (2007a) put forward a solution and studied the cosmic duality in quintom universe. According to Cai et al. (2007a), we draw a simplified version for the scalar field. For the quintessence field, it is given by

$$\phi(t) \sim \sqrt{2}\ln|t|, \tag{9}$$

where the scalar factor $a \propto t$. Thus, we have $a = k_1 t$, where the coefficient k_1 is a constant. By $a = \frac{1}{1+z}$, we ultimately have

$$\dot{\phi}^2 = 2H_0^2 k_1^2 (1+z)^2. \tag{10}$$

While for the phantom field, we assume

$$\sigma(t) \sim \sqrt{2}t, \tag{11}$$

where scalar factor $a \propto \exp(t^2/2)$. In virtue of a factor k_2, we can also obtain $a = k_2 \exp(t^2/2)$. Similarly, we have

$$\dot{\sigma}^2 = 2H_0^2. \tag{12}$$

For the quintom field, we consider two categories, namely quintessence field changing into phantom field (hereafter quintomA), and phantom field changing into quintessence field (hereafter quintomB). Last, according to the initial condition $H(z=0)/H_0 = 1$, we have $k_1^2 = \frac{1}{2}(1 - \Omega_{m0})(1 + w_0)$ for quintessence scalar field.

3. Observational Data

3.1. Type Ia Supernovae

The latest Type Ia supernova data we use are Pantheon sample from Scolnic et al. (2018), which consists 1048 data points. For these samples, their redshifts have a wide span of $0.01 < z < 2.3$. For each SN Ia, the observed distance modulus is given by

$$\mu_{\rm obs} = m_B^\star + \mathcal{M}, \tag{13}$$

where $m_B^\star$ is the observed peak magnitude in rest frame B band. The quantity $\mathcal{M}$ is the nuisance parameter. The full covariance matrix Cov of the Pantheon sample is given by

$$\text{Cov} = \boldsymbol{D}_{\rm stat} + \boldsymbol{C}_{\rm sys}. \tag{14}$$

Here matrix $\boldsymbol{D}_{\rm stat}$ is the diagonal part of the statistical uncertainty. The $\boldsymbol{C}_{\rm sys}$ is the systematic covariance matrix between peak magnitude. They are available in the catalogs of Pan-STARRS.[3]

The theoretical distance modulus is usually estimated as

$$\mu_{\rm th}(z) = 5\log_{10} D_L(z) + \mathcal{M}, \tag{15}$$

where the luminosity distance is

$$D_L(z) = (1 + z_{\rm hel})\int_0^{z_{\rm cmb}} \frac{H_0 d\tilde{z}}{H(\tilde{z})}. \tag{16}$$

Finally, the cosmological parameter can be estimated by the chi-squared function

$$\chi^2 = \Delta\mu \text{Cov}^{-1}\Delta\mu^T, \tag{17}$$

where $\Delta\mu = \mu_{\rm obs} - \mu_{\rm th}$.

3.2. Baryon Acoustic Oscillations

The BAO data we use here are 15 latest transversal BAO measurements (Nunes et al. 2020), $\theta_{\rm BAO}(z)$. They are obtained through the BAO signal position in the 2PACF, a model-independent approach (Jassal et al. 2005; Blake et al. 2011). There is not a fiducial cosmological model assumption, comparing with the traditional BAO measurement. Their inclusion can break the degeneracy of dark energy model parameters, and improve the constraints significantly (Hernández-Almada et al. 2021; Motta et al. 2021). The theoretical angular scale is evaluated by

$$\theta_{\rm th}(z) = \frac{r_{\rm drag}}{(1+z)D_A(z)}, \tag{18}$$

where $D_A(z) = D_L/(1+z)^2$ is the angular diameter distance, $r_{\rm drag}$ is the sound horizon at baryon drag epoch (Aghanim et al. 2020). The parameters can be estimated by

$$\chi^2_{\rm BAO} = \sum_{i=1}^{15}\left(\frac{\theta_{\rm BAO}(z_i) - \theta_{\rm th}(z_i)}{\sigma_i}\right)^2, \tag{19}$$

where σ_i is the error of traditional BAO data.

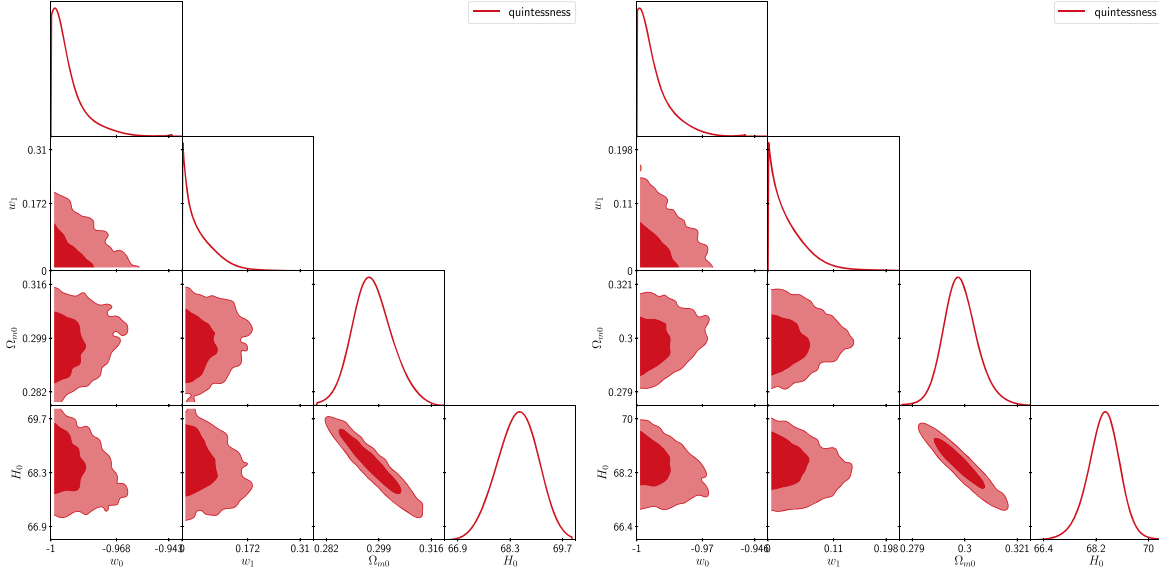[3] https://archive.stsci.edu/prepds/ps1cosmo/index.html

Figure 1. Posterior distributions of the cosmological parameters in quintessence field for fractional form $w = w_0 + w_1 \frac{z}{(1+z)^2}$ (left) and logarithmic form $w = w_0 + w_1 \frac{\ln(1+z)}{1+z}$ model (right) using all the data sets.

3.3. Cosmic Microwave Background

The CMB has become one of the most powerful ways to study the cosmology and the physics of early universe. According to the Planck 2018 (Aghanim et al. 2020), we use the full temperature and polarization angular power-spectrum data from Planck 2018. Specifically, they are respectively `Plik` likelihood, a combination of Planck TT,TE,EE spectra at $\ell > 29$, temperature-only `Commander` likelihood named `Planck_lowl_TT` at low multipole $2 \leqslant \ell \leqslant 29$, and low multipole $2 \leqslant \ell \leqslant 29$ EE likelihood named Planck_lowl_EE from `SimAll`.

3.4. Observational Hubble Parameter

$H(z)$ is a direct measurement of the cosmic expansion rate, which can be obtained via the differential ages of passively evolving galaxies (Simon et al. 2005; Jimenez & Loeb 2008; Stern et al. 2010)

$$H(z) = -\frac{1}{1+z}\frac{dz}{dt}. \tag{20}$$

This method is also called cosmic chronometer. In our recent work (Zhang & Xia 2016), we used 30 cosmic chronometer data and studied the dark energy, finding a powerful constraint. Cosmological parameters can be constrained by the observational Hubble parameter data via

$$\chi^2_{H(z)} = \sum_{i=1}^{30}\left(\frac{H_{\text{th}}(z_i) - H_{\text{obs}}(z_i)}{\sigma_i^2}\right)^2. \tag{21}$$

4. Observational Constraints and Analysis

4.1. Constraints from all Samples

We obtain cosmological parameter constraints using the Einstein–Boltzmann code `CLASS-PT` (Chudaykin et al. 2020) interfaced with the `Montepython` Monte Carlo sampler (Audren et al. 2013; Brinckmann & Lesgourgues 2019). We use the Python module basing on the Markov chain Monte Carlo approach, to perform the corresponding χ^2 statistics.

For the quintessence scalar field, we present the corresponding results in Table 1 and Figure 1. For the fractional form model with $w = w_0 + w_1 z/(1+z)^2$, the data sets present slightly moderate matter density parameter $\Omega_{m0} = 0.297 \pm 0.007$. For the dark energy, current equation of state is $w_0 = -0.991^{+0.002}_{-0.008}$. Moreover, parameter w_1 is also insignificant. However, for the Hubble constant we have been focused on, its value is relatively small, namely $H_0 = 68.5^{+0.594}_{-0.557}$ km s^{-1} Mpc^{-1}. Comparing with the R20, it presents a 3.31σ tension, which is rather severe. Turn to the second model, logarithmic form, we find that the corresponding constraints are similar as the former model. As shown in Figure 1, dark energy parameters w_0 and w_1 are constrained with a low level. Only a bound for them can be obtained. For the important Hubble constant, this model still cannot give an ideal solution. That is, Hubble constant is $H_0 = 68.4^{+0.646}_{-0.515}$ km s^{-1} Mpc^{-1}, which is similar as the result in the first model. Hubble tension in this model has reached 3.37σ. In short, we cannot optimistically believe that quintessence field

Table 1
Constraints of Cosmological Parameters at 68% C.L. for Different Models Using all the Observational Data Sets

	Model	$100\Omega_b h^2$	$\Omega_c h^2$	Ω_{m0}	w_0	w_1	H_0	Tension	$|\ln B_{i0}|$
quintessence	$w = w_0 + w_1 \frac{z}{(1+z)^2}$	2.2638 ± 0.0158	0.116 ± 0.00112	0.297 ± 0.007	$-0.991^{+0.002}_{-0.008}$	$0.046^{+0.009}_{-0.046}$	$68.5^{+0.594}_{-0.557}$	3.31σ	8.98
	$w = w_0 + w_1 \frac{\ln(1+z)}{1+z}$	2.2590 ± 0.0140	0.116 ± 0.00115	0.298 ± 0.008	$-0.992^{+0.002}_{-0.008}$	$0.036^{+0.006}_{-0.036}$	$68.4^{+0.646}_{-0.515}$	3.37σ	5.95
phantom	$w = w_0 + w_1 \frac{z}{(1+z)^2}$	2.2434 ± 0.0140	0.118 ± 0.00124	0.280 ± 0.007	$-1.030^{+0.033}_{-0.008}$	$-0.45^{+0.266}_{-0.248}$	$71.2^{+0.849}_{-0.874}$	1.28σ	29.45
	$w = w_0 + w_1 \frac{\ln(1+z)}{1+z}$	2.2449 ± 0.0151	0.118 ± 0.00138	0.279 ± 0.007	$-1.030^{+0.031}_{-0.006}$	$-0.41^{+0.222}_{-0.206}$	$71.3^{+0.854}_{-0.917}$	1.20σ	31.89
quintomA	$w = w_0 + w_1 \frac{z}{(1+z)^2}$	2.2522 ± 0.0153	0.118 ± 0.00130	0.282 ± 0.008	$-1.260^{+0.044}_{-0.034}$	$1.160^{+0.027}_{-0.163}$	$70.7^{+0.894}_{-0.907}$	1.57σ	17.65
	$w = w_0 + w_1 \frac{\ln(1+z)}{1+z}$	2.2530 ± 0.0143	0.118 ± 0.00124	0.283 ± 0.008	$-1.190^{+0.042}_{-0.034}$	$0.643^{+0.025}_{-0.143}$	$70.7^{+0.914}_{-0.889}$	1.59σ	15.97
quintomB	$w = w_0 + w_1 \frac{z}{(1+z)^2}$	2.2442 ± 0.0137	0.119 ± 0.00134	0.286 ± 0.007	$-0.655^{+0.894}_{-0.125}$	$-2.84^{+0.894}_{-0.804}$	$70.6^{+0.804}_{-0.858}$	1.69σ	26.82
	$w = w_0 + w_1 \frac{\ln(1+z)}{1+z}$	2.2418 ± 0.0133	0.119 ± 0.00115	0.285 ± 0.008	$-0.704^{+0.096}_{-0.116}$	$-2.09^{+0.662}_{-0.512}$	$70.8^{+0.881}_{-0.922}$	1.52σ	29.72

Note. The parameter H_0 is measured in units of $\mathrm{km\,s^{-1}\,Mpc^{-1}}$.

relaxes or solves the Hubble tension, in these two types of parameterization of equation of state of the dark energy.

For the phantom scalar field, the constraints improve greatly. In the first fractional form, the matter density parameter is $\Omega_{m0} = 0.280 \pm 0.007$, which is slightly smaller than the constraint in quintessence field. For the parameters of equation of state, they are better than the constraints in quintessence scalar field, as shown in Figure 2. Similarly, current equation of state is $w_0 = -1.030^{+0.033}_{-0.008}$, which is also close to the cosmological constant. Importantly, we find that Hubble constant tension has been improved obviously. To be specific, Hubble constant is $H_0 = 71.2^{+0.849}_{-0.874}$ km s^{-1} Mpc^{-1} with about 1.2% uncertainty. Going back to the Hubble tension problem, the tension has been reduced to 1.28σ. For the logarithmic form, the corresponding constraints are also much better than the quintessence scalar field. Especially, the Hubble tension can reduce to 1.20σ.

For the quintomA and quintomB scalar field, we respectively consider transformation between quintessence field and phantom field, as shown in Figures 3 and 4. For the matter density, parameter Ω_{m0} still can be obtained with a high precision. For the equation of state, parameters w_0 and w_1 deviate from the cosmological constant significantly, which is different from the results in quintessence field and phantom field. For the Hubble constant, they present a better constraint than the quintessence field. However, the tension still locates at $1.52\sigma - 1.69\sigma$.

In short, we find that Hubble tension in the phantom scalar field is the smallest. Moreover, it is little affected by the dark energy parameterization.

4.2. Bayesian Evidence

In this section, we would seek which model is more effective, compared with the standard ΛCDM cosmology. This statistical comparison can be realized through the Bayesian

evidence. Here we use the publicly available code MCEvidence (Heavens et al. 2017a, 2017b) to compute the evidence of the model. It is very convenient because of its only usage of MCMC chains.

According to the Bayes' theorem, we can describe the probability that cosmological model $\mathcal{M}$ is true as:

$$P(\mathcal{M}|d) = \frac{P(d|\mathcal{M})}{P(d)}P(\mathcal{M}) = \frac{P(d|\mathcal{M})}{\sum P(d|\mathcal{M}_i)P(\mathcal{M}_i)}P(\mathcal{M}) \tag{22}$$

where $P(\mathcal{M})$ and $P(\mathcal{M}|d)$ are the prior probability and posterior probability, d are the observational data, respectively.

Considering two models, $\mathcal{M}_0$ and $\mathcal{M}_i$, above posterior probability of these two models have the relationship

$$\frac{P(\mathcal{M}_i|d)}{P(\mathcal{M}_0|d)} = \frac{P(d|\mathcal{M}_i)P(\mathcal{M}_i)}{P(d|\mathcal{M}_0)P(\mathcal{M}_0)} = B_{i0}\frac{P(\mathcal{M}_i)}{P(\mathcal{M}_0)}, \tag{23}$$

where B_{i0} is the Bayes factor

$$B_{i0} \equiv \frac{P(d|\mathcal{M}_i)}{P(d|\mathcal{M}_0)}. \tag{24}$$

Generally, the cosmological model $\mathcal{M}_0$ is adopted as the standard ΛCDM model. The Bayes factor $B_{i0} > 1$ or $B_{i0} < 1$ indicates whether the observational data prefer model $\mathcal{M}_i$ rather than $\mathcal{M}_0$ or not. According to the Jeffreys' scale (Trotta 2008), we can use the factor $|\ln B_{i0}|$ to test the evidence for the model $\mathcal{M}_i$, as shown in Table 2. Obviously, the larger the factor $|\ln B_{i0}|$, the more support for the model $\mathcal{M}_i$. Compared with the standard ΛCDM model, the Bayes factors in all considered scalar fields can be calculated, as shown in Table 1. We find that the Bayes factor $|\ln B_{i0}|$ in the phantom scalar field and quintomB field have larger values. That is, the observational data more favor these two kinds of models. By further comparison, we find that the phantom field has the largest Bayes factor. Theoretically, the phantom scalar field is more effective.
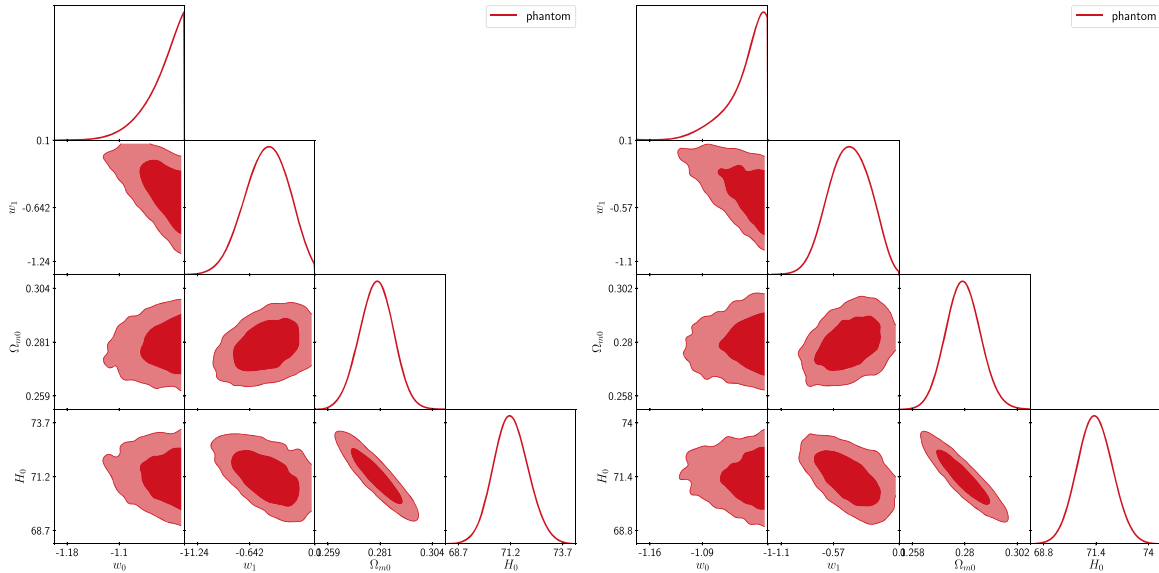
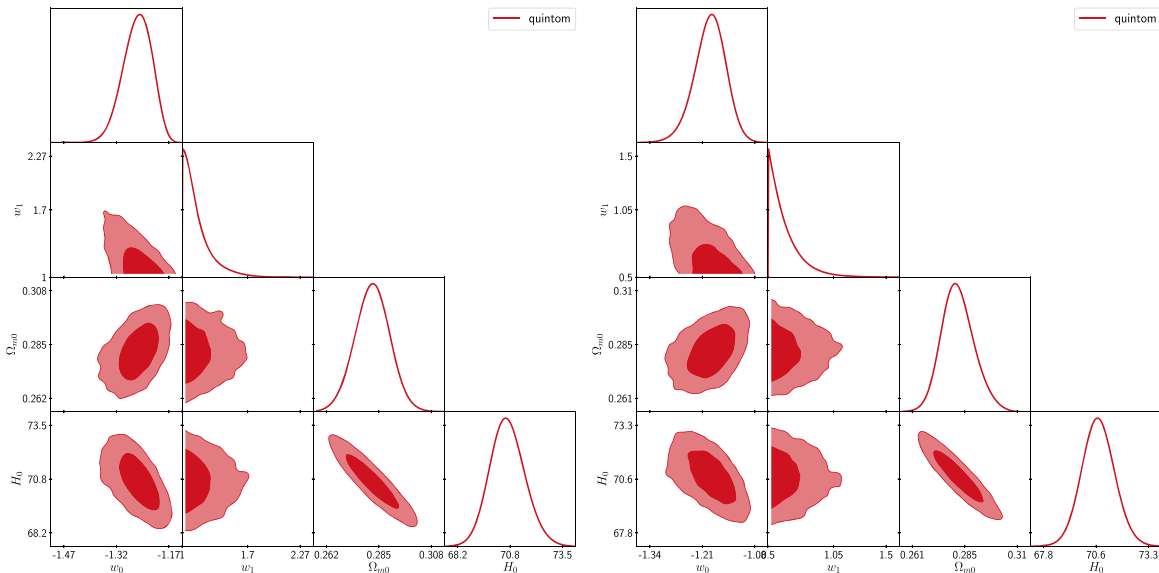**Figure 2.** The same as Figure 1 but for phantom field.

Figure 3. The same as Figure 1 but for quintomA field.

4.3. A Reason for the Hubble Tension

To test the reason for the Hubble tension, we perform a comparison on the probability density of $\Omega_b h^2$, $\Omega_c h^2$ and $\Omega_{m0} h^2$ for different dark energy models, as shown in Figure 5. We also analyze a possible physical phenomenon of the low tension from the kinematics, which expect to provide a new understanding of the Hubble tension.

The matter density has an important effect on the CMB spectra. It affects the amount of lensing in the CMB spectra and the amplitude of the CMB-lensing reconstruction spectrum. From the Planck 2018 release, it is obtained $\Omega_{m0} h^2 = 0.1432 \pm 0.0013$ (Aghanim et al. 2020). As shown in Figure 24 of this reference, the Planck Collaboration investigated the *TT* power spectrum residuals over the value of $\Omega_{m0} h^2$. They found that a less lensing is allowed by a lower
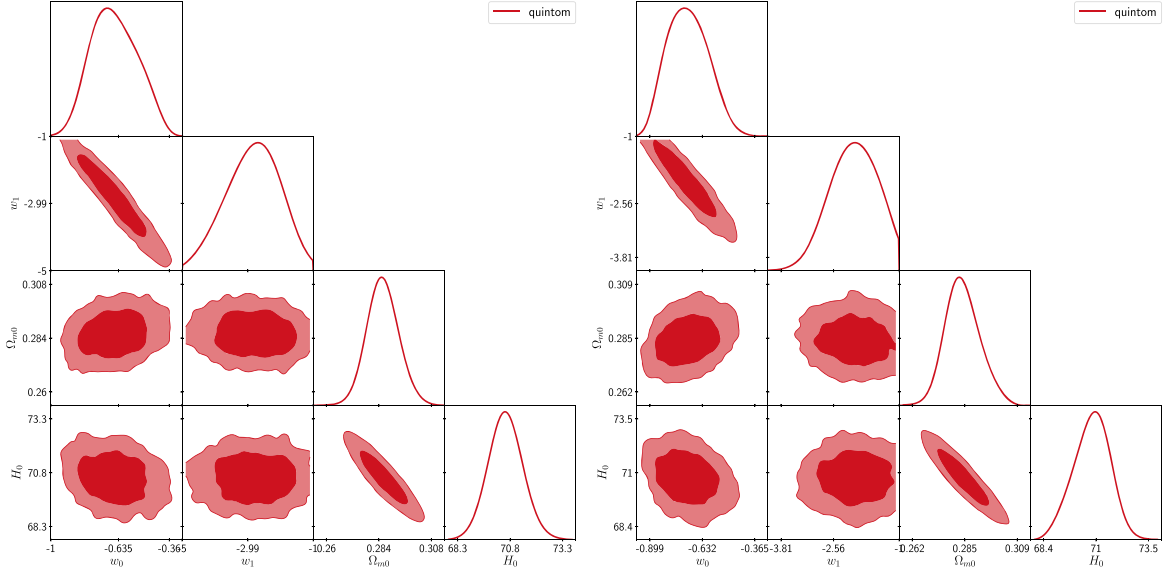
Figure 4. The same as Figure 1 but for quintomB field.

Table 2
Bayes Factor in the Revised Jeffreys' Scale

$|\ln B_{i0}|$	Evidence for Model $\mathcal{M}_i$
$0 < |\ln B_{i0}| < 1$	weak
$1 < |\ln B_{i0}| < 3$	positive
$3 < |\ln B_{i0}| < 5$	strong
$5 < |\ln B_{i0}|$	very strong

$\Omega_{m0}h^2$. Hence a larger oscillatory residual can be given. In Figure 5, we compare the parameters $\Omega_b h^2$, $\Omega_c h^2$ and $\Omega_{m0}h^2$ for different dark energy models. First, we find that density parameter $\Omega_b h^2$ in these scalar fields are larger than the value in standard ΛCDM model. Especially, density $\Omega_b h^2$ in the quintessence scalar field is farthest from the standard ΛCDM model. Moreover, we find that the phantom field closest to the standard ΛCDM model. Second, in the middle panel of Figure 5, we find that quintessence scalar field still deviates from the standard value farthest. For parameter $\Omega_c h^2$, the phantom field slightly deviates from the standard ΛCDM model. Finally, we find that density parameter $\Omega_{m0}h^2$ in the phantom field is still closest to the standard ΛCDM model. Therefore, we are in a dilemma. That is, the phantom scalar field can better solve the Hubble tension, but the corresponding density parameters are closest to the standard ΛCDM model. This similarity makes it difficult to distinguish them.

As pointed out in previous work (Linares Cedeño et al. 2021), the Hubble tension can be reconciled is because a dark energy model with phantom-like EoS can generate extra acceleration of the universe, when compared with the fiducial

ΛCDM model. Their result is consistent with our work. In order to further reveal the reason why Hubble tension can be reconciled in this scenario, we investigate the kinematic $\ddot{a}$ in Figure 6. First, we find that acceleration $\ddot{a}$ in these scalar fields is similar at about redshift $z > 0.5$. Moreover, they are much similar as the ΛCDM model. However, for low redshift, we should notice that the $\ddot{a}$ deviates from each other, especially in the near future. More importantly, we note that the $\ddot{a}$ for the phantom scalar field decreases in the future, while for the other field, the $\ddot{a}$ increases in the future. In our knowledge, this is the first time discovering this interesting physical phenomenon.

5. Conclusion and Discussion

Hubble tension has become a key problem in cosmology. It even implies a possibility of new physics or the failure of immortal ΛCDM model. In this paper, we consider three scalar fields as the dark energy to reconcile the Hubble tension. The scalar fields we consider are quintessence field, phantom field and quintom field. The observational data sets, SN Ia from Pantheon samples, transversal BAO measurement, CMB power spectra and $H(z)$ data. The constraints indicate that phantom field can reconcile the Hubble tension to 1.20σ. We also perform a model comparison using the Bayes factor from the public code `MCEvidence`. The comparison shows that phantom scalar field is still the most effective in these models.

To investigate the reason of the Hubble tension, we perform a series of analysis. From the probability density in Figure 5, we find that the scalar fields provide a bigger $\Omega_b h^2$ and a lower $\Omega_c h^2$, when compared with the standard ΛCDM model.
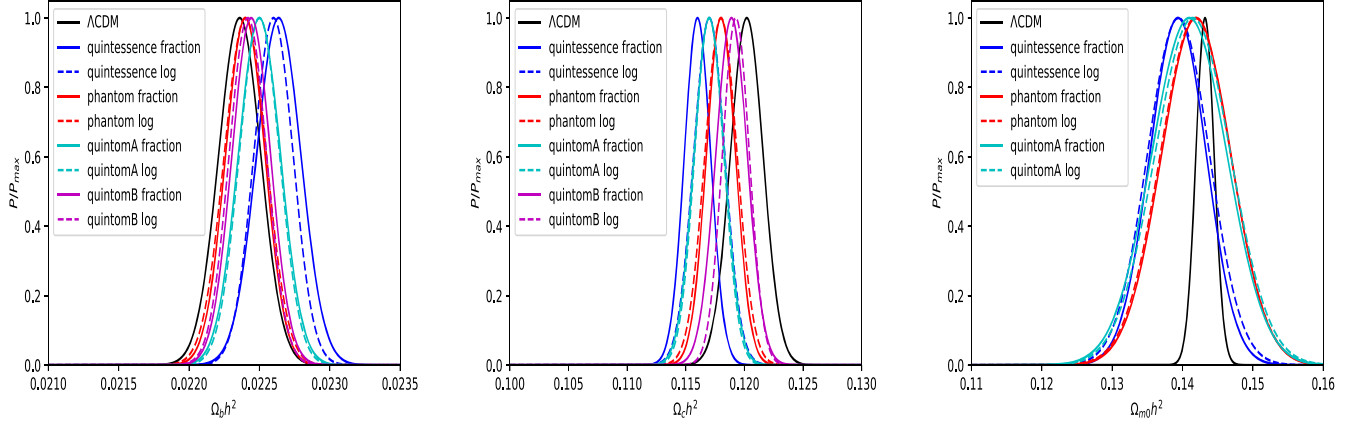
Figure 5. Probability density of $\Omega_b h^2$, $\Omega_c h^2$ and $\Omega_{m0} h^2$ for different models.
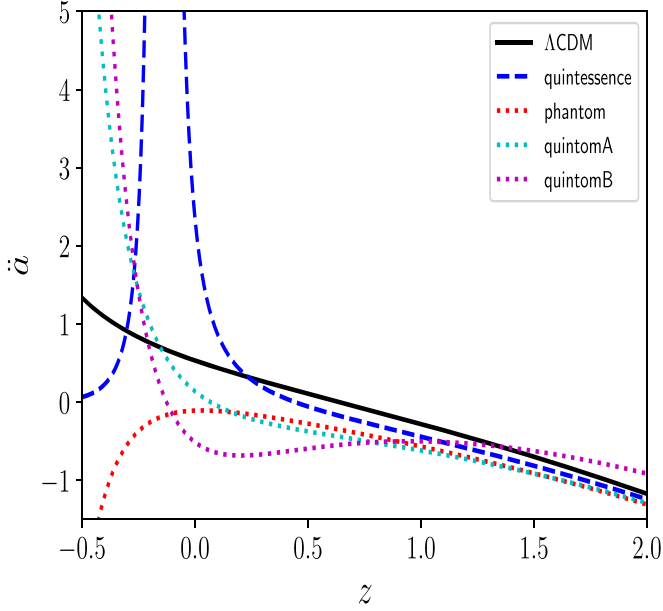

Figure 6. Comparison of the kinematics $\ddot{a}$ for different models.

Moreover, the phantom field has a $\Omega_b h^2$ closest to the standard ΛCDM model. It can affect the CMB-lensing spectrum (Aghanim et al. 2020) and provide an energy transformation between dark matter and dark energy (Di Valentino et al. 2020; Yang et al. 2020).

A numerous of previous works (Di Valentino et al. 2016, 2021b; Yang et al. 2019; Alestas et al. 2020; Vagnozzi 2020) find that a phantom-like dark energy can reconcile the Hubble tension. To further reveal the reason, we investigate the kinematic $\ddot{a}$ in Figure 6. We find that acceleration $\ddot{a}$ in these scalar fields is similar to the standard ΛCDM model at redshift $z > 0.5$. However, for low redshift, we should notice that the $\ddot{a}$ deviates from each other, especially

in the near future. For the phantom scalar field, we note that the $\ddot{a}$ decreases in the future. While for the other field, the $\ddot{a}$ increases in the future. This interesting physical phenomenon was discovered for the first time.

We reconstruct the potential V via a different approach. Traditionally, the potential was usually parameterized for the scalar field, such as power form, exponential form, trigonometric function etc. However, this artificial method makes it very difficult to constrain the Hubble constant, because H_0 is commonly coupled in the potential. Fortunately, parameterization of dark energy w can bypass this difficulty. Moreover, the Hubble tension can be reconciled with a better level.

Besides the traditional measurements, some trendy observations are also on the way. The first Hubble constant given by the gravitational-waves (GW) GW170817 event with its electromagnetic signals is $H_0 = 70.0^{+12.0}_{-8.0}$ km s^{-1} Mpc^{-1} (The LIGO Scientific Collaboration et al. 2017). However, introducing the peculiar motion correction of the GW source, GW170817 event combining with interferometry observation gives $H_0 = 68.3^{+4.6}_{-4.5}$ km s^{-1} Mpc^{-1} (Mukherjee et al. 2021). Recently, Cao et al. (2022) investigated this tension by the gravitational waves and strong gravitational lensing. They found that constraint of H_0 from 700 simulated GW events would exceed that of the Planck 2018 results. Considering 1000 GW events by the Einstein Telescope, it will provide a much tighter constraint on H_0 with 0.5% uncertainty. Therefore, future multi-messenger astronomy will be a very exciting program in understanding the Hubble tension. Besides that, strongly lensed type Ia supernovae are also expected to have some advantages in measuring Hubble constant with uncertainty $\Delta H_0 = 0.26$ km s^{-1} Mpc^{-1} (Qi et al. 2022). Fast radio bursts, radio signal with high energy and brightness, will open a new window to our cosmology (Wei et al. 2018; Zhao et al. 2020; Qiu et al. 2021). Using the Fast Radio Bursts, Hagstotz et al. (2021) obtained a new measurement $H_0 = 62.3 \pm 9.1$ km s^{-1} Mpc^{-1}. Fortunately, with the help of high

sensitivity of the Five-hundred-meter Aperture Spherical Radio Telescope (Zhu et al. 2020), high precision of the Hubble constant H_0 can be expected.

Acknowledgments

References

Aghanim, N., Akrami, Y., Ashdown, M., et al. 2020, A&A, 641, A6
Alestas, G., Kazantzidis, L., & Perivolaropoulos, L. 2020, PhRvD, 101, 123516
Audren, B., Lesgourgues, J., Benabed, K., & Prunet, S. 2013, JCAP, 2013, 001
Blake, C., Brough, S., Colless, M., et al. 2011, MNRAS, 415, 2876
Brinckmann, T., & Lesgourgues, J. 2019, PDU, 24, 100260
Cai, Y.-F., Li, H., Piao, Y.-S., & Zhang, X. 2007a, PhLB, 646, 141
Cai, Y.-f., Li, M.-z., Lu, J.-X., et al. 2007b, PhLB, 651, 1
Cai, Y.-F., Saridakis, E. N., Setare, M. R., & Xia, J.-Q. 2010, PhR, 493, 1
Cao, M.-D., Zheng, J., Qi, J.-Z., Zhang, X., & Zhu, Z.-H. 2022, ApJ, 934, 108
Chudaykin, A., Ivanov, M. M., Philcox, O. H. E., & Simonović, M. 2020, PhRvD, 102, 063533
Di Valentino, E., Linder, E. V., & Melchiorri, A. 2020, PDU, 30, 100733
Di Valentino, E., Melchiorri, A., Mena, O., & Vagnozzi, S. 2020, PhRvD, 101, 063502
Di Valentino, E., Melchiorri, A., & Silk, J. 2016, PhLB, 761, 242
Di Valentino, E., Mena, O., Pan, S., et al. 2021a, CQGra, 38, 153001
Di Valentino, E., Mukherjee, A., & Sen, A. A. 2021b, Entrp, 23, 404
Freedman, W. L. 2017, NatAs, 1, 0121
Freedman, W. L. 2021, ApJ, 919, 16
Hagstotz, S., Reischke, R., & Lilow, R. 2021, arXiv:2104.04538
Heavens, A., Fantaye, Y., Mootoovaloo, A., et al. 2017a, arXiv:1704.03472
Heavens, A., Fantaye, Y., Sellentin, E., et al. 2017b, PhRvL, 119, 101301
Hernández-Almada, A., García-Aspeitia, M. A., Rodríguez-Meza, M. A., & Motta, V. 2021, EPJC, 81, 295
Hubble, E., & Humason, M. L. 1931, ApJ, 74, 43
Jassal, H. K., Bagla, J. S., & Padmanabhan, T. 2005, MNRAS, 356, L11
Jimenez, R., & Loeb, A. 2008, ApJ, 573, 37
Leavitt, H. S., & Pickering, E. C. 1912, HarCi, 173, 1
Li, X., & Shafieloo, A. 2019, ApJL, 883, L3
Linares Cedeño, F. X., Roy, N., & Ureña López, L. A. 2021, PhRvD, 104, 123502
Motta, V., García-Aspeitia, M. A., Hernández-Almada, A., Magaña, J., & Verdugo, T. 2021, Univ, 7, 163
Mukherjee, S., Lavaux, G., Bouchet, F. R., et al. 2021, A&A, 646, A65
Niedermann, F., & Sloth, M. S. 2020, PhRvD, 102, 063527
Nunes, R. C., Yadav, S. K., Jesus, J. F., & Bernui, A. 2020, MNRAS, 497, 2133
Pan, S., Yang, W., Di Valentino, E., Shafieloo, A., & Chakraborty, S. 2020, JCAP, 06, 062
Qi, J.-Z., Cui, Y., Hu, W.-H., et al. 2022, PhRvD, 106, 023520
Qiu, X.-W., Zhao, Z.-W., Wang, L.-F., Zhang, J.-F., & Zhang, X. 2021, arXiv:2108.04127
Riess, A. G., Casertano, S., Yuan, W., et al. 2021, ApJL, 908, L6
Sahni, V. 2004, The Physics of the Early Universe (Berlin: Springer), 141
Scolnic, D. M., Jones, D. O., Rest, A., et al. 2018, ApJ, 859, 101
Simon, J., Verde, L., & Jimenez, R. 2005, PhRvD, 71, 123001
Stern, D., Jimenez, R., Verde, L., Kamionkowski, M., & Stanford, S. A. 2010, JCAP, 2010, 008
The LIGO Scientific CollaborationThe Virgo CollaborationThe 1M2H Collaboration, et al. 2017, Natur, 551, 85
Trotta, R. 2008, ConPh, 49, 71
Vagnozzi, S. 2020, PhRvD, 102, 023518
Wei, J.-J., Wu, X.-F., & Gao, H. 2018, ApJL, 860, L7
Wu, Q., Zhang, G. Q., & Wang, F. Y. 2021, arXiv:2108.00581
Yang, W., Di Valentino, E., Mena, O., & Pan, S. 2020, PhRvD, 102, 023535
Yang, W., Di Valentino, E., Pan, S., Shafieloo, A., & Li, X. 2021a, PhRvD, 104, 063521
Yang, W., Di Valentino, E., Pan, S., Wu, Y., & Lu, J. 2021b, MNRAS, 501, 5845
Yang, W., Pan, S., Di Valentino, E., Saridakis, E. N., & Chakraborty, S. 2019, PhRvD, 99, 043543
Ye, G., Zhang, J., & Piao, Y.-S. 2021, arXiv:2107.13391
Zhang, M.-J., & Li, H. 2018, EPJC, 78, 460
Zhang, M.-J., & Xia, J.-Q. 2016, JCAP, 12, 005
Zhao, G.-B., Xia, J.-Q., Li, M., Feng, B., & Zhang, X. 2005, PhRvD, 72, 123515
Zhao, S., Liu, B., Li, Z., & Gao, H. 2021, ApJ, 916, 70
Zhao, Z.-W., Li, Z.-X., Qi, J.-Z., et al. 2020, ApJ, 903, 83
Zhu, W., Li, D., Luo, R., et al. 2020, ApJL, 895, L6